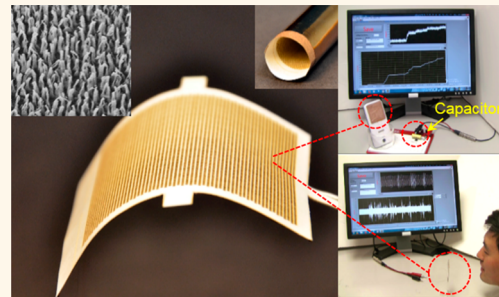


# Ultrathin, Rollable, Paper-Based Triboelectric Nanogenerator for Acoustic Energy Harvesting and Self-Powered Sound Recording

Xing Fan,<sup>†,‡,||</sup> Jun Chen,<sup>†,||</sup> Jin Yang,<sup>†,||</sup> Peng Bai,<sup>†</sup> Zhaoling Li,<sup>†</sup> and Zhong Lin Wang<sup>\*,§</sup>

<sup>†</sup>School of Materials Science and Engineering, Georgia Institute of Technology, Atlanta, Georgia 30332-0245, United States, <sup>‡</sup>College of Chemistry and Chemical Engineering, Chongqing University, Chongqing 400044, P. R. China, and <sup>§</sup>Beijing Institute of Nanoenergy and Nanosystems, Chinese Academy of Sciences, Beijing 100083, P. R. China. <sup>||</sup>X.F., J.C., and J.Y. contributed equally to this work.

**ABSTRACT** A 125  $\mu\text{m}$  thickness, rollable, paper-based triboelectric nanogenerator (TENG) has been developed for harvesting sound wave energy, which is capable of delivering a maximum power density of 121 mW/m<sup>2</sup> and 968 W/m<sup>3</sup> under a sound pressure of 117 dB<sub>SPL</sub>. The TENG is designed in the contact-separation mode using membranes that have rationally designed holes at one side. The TENG can be implemented onto a commercial cell phone for acoustic energy harvesting from human talking; the electricity generated can be used to charge a capacitor at a rate of 0.144 V/s. Additionally, owing to the superior advantages of a broad working bandwidth, thin structure, and flexibility, a self-powered microphone for sound recording with rolled structure is demonstrated for all-sound recording without an angular dependence. The concept and design presented in this work can be extensively applied to a variety of other circumstances for either energy-harvesting or sensing purposes, for example, wearable and flexible electronics, military surveillance, jet engine noise reduction, low-cost implantable human ear, and wireless technology applications.



**KEYWORDS:** paper-thin · rollable · triboelectric nanogenerator · acoustic energy harvesting · self-powered sound recording

The serious energy shortage can be a major factor that limits the quality of life.<sup>1–6</sup> Vast amounts of acoustic energy from human talking, traffic noise, music, and so forth are ubiquitous but regrettably being ignored. Acoustic energy harvesting has not been as popular as other types of energy harvesting, and does not get extensively explored or well utilized, which is not only attributed to its much lower power density but also a lack of effective harvesting technology. Currently, the mechanisms of acoustic energy harvesting are limited to transductions based on piezoelectric effect, electrostatic effect, and triboelectric effect.<sup>7–10</sup> Wide range usage of these techniques is limited by factors such as low efficiency, high structure complexity, and large volumes due to the required resonance cavity that results in extremely low volume specific energy.<sup>11–14</sup>

In this work, innovatively employing arrays of microholes for acoustic response

enhancement, an ultrathin, rollable, paper-based acoustic energy harvester is demonstrated. Relying on the coupling effect of triboelectrification and electrostatic induction, the as-fabricated triboelectric nanogenerator (TENG), with a thickness of 125  $\mu\text{m}$ , is capable of delivering a maximum power density of 121 mW/m<sup>2</sup> (volume power density of 968 W/m<sup>3</sup>) under a sound pressure of 117 dB<sub>SPL</sub>. The superior feature due to the structural novelty enables it to harvest acoustic energy from portable electronics. The energy harvested from human talking over a cell phone can charge a capacitor at a rate of 0.144 V/s. Furthermore, with a collection of compelling features, such as broad working bandwidth, structural rollability, and directional independence, the as-prepared paper based nanogenerator is capable of serving as a self-powered sensor<sup>15–20</sup> for sound recording. The concept and design presented in this work can be extensively applied in a variety of other

\* Address correspondence to zhong.wang@mse.gatech.edu.

Received for review January 28, 2015 and accepted March 19, 2015.

Published online  
10.1021/acsnano.5b00618

© XXXX American Chemical Society

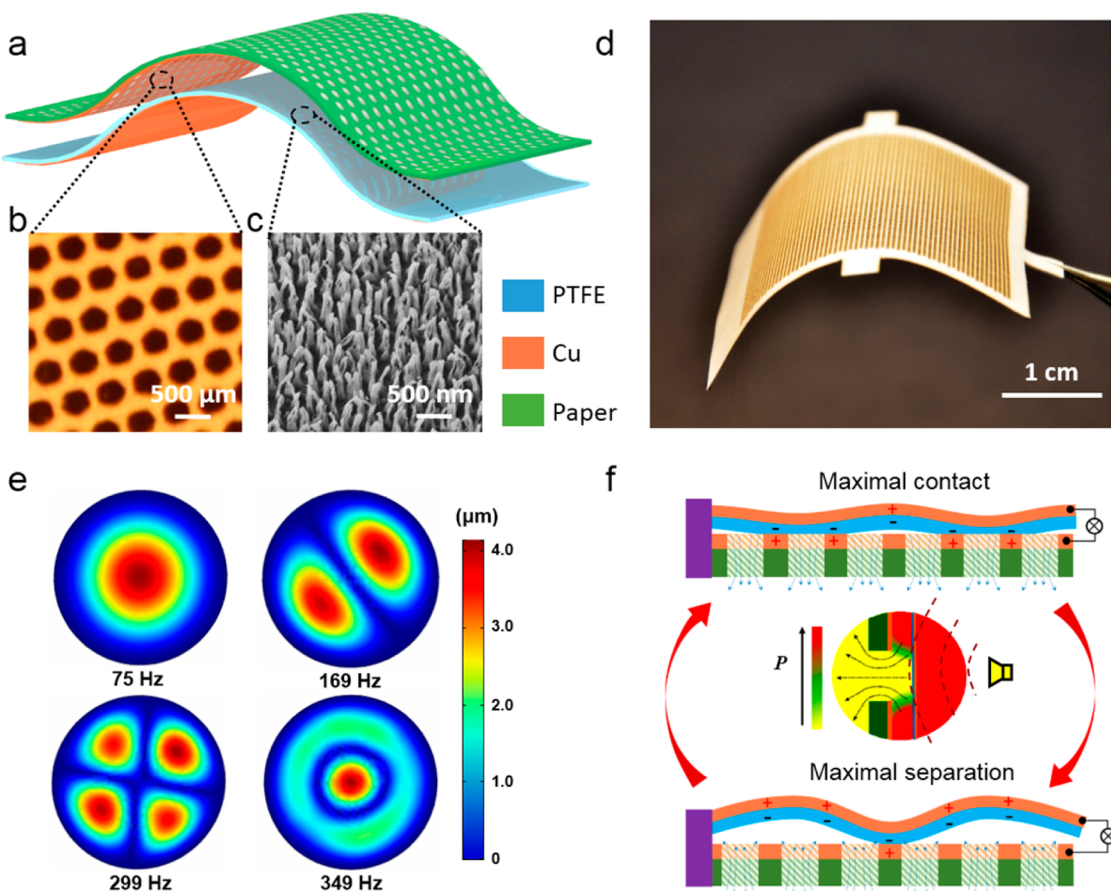


**Figure 1.** Structural design and operating principle of the ultrathin paper-based TENG. (a) Schematic illustrations of the paper-based TENG. (b) Photograph of the multihole paper electrode. (c) SEM image of the PTFE polymer nanowires. (d) Photograph of an as-fabricated paper-based TENG. (e) The ANSYS software was employed to characterize the PTFE membrane vibration under various sound frequencies. (f) Illustration to interpret the sound wave induced PTFE membrane vibration and electricity generation.

circumstances for either energy-harvesting or sensing purposes, for example, wearable and flexible electronics, military surveillance, jet engine noise reduction, low-cost implantable human ear, and wireless technology applications.

## RESULTS AND DISCUSSION

An ultrathin triboelectric nanogenerator (TENG) has a multilayered structure composed of thin film materials that are vertically laminated. A layer of multiholed paper forms the structural backbone of the TENG, which was coated with copper acting as an electrification layer that generates triboelectric charges upon contacting with a thin polytetrafluoroethylene (PTFE) membrane,<sup>21–23</sup> as schematically shown in Figure 1a. Papers were selected as the structural materials owing to its flexibility, lightweight, good machinability, low cost, as well as biodegradability. Of course, instead of papers, other expensive organic thin films can be chosen as well. For the purpose of enhancing a broadband acoustic response, holes with diameters of 400  $\mu\text{m}$  were evenly punched and distributed on the paper substrate. A photograph of the multihole paper electrode is demonstrated in Figure 1b. In order to

enhance the triboelectrification, the polymer nanowires array was purposely created onto the PTFE membrane,<sup>24–29</sup> as shown in the scanning electron microscopy (SEM) image in Figure 1c. Figure 1d is a photograph of an as-fabricated paper-based TENG with a thickness less than 125  $\mu\text{m}$ .

The working principle of the paper-thin triboelectric nanogenerator can be elucidated from two aspects, namely, sound induced membrane vibration and vibration induced electricity generation. On one hand, when an external sound wave is continuously incident onto the paper-thin TENG, the flexible PTFE membrane would vibrate accordingly. Namely, the propagation of the sound wave will cause a periodical air-pressure difference between two sides of the membrane, which leads to the membrane vibration. This vibrational mechanism is distinctly different from the traditional acoustic energy harvester that relies on a resonator cavity, for which the mechanical vibration is attributed to the alternative air compression–expansion within the cavity.<sup>9,13,14</sup> The ANSYS software is employed to simulate the sound wave induced PTFE membrane vibration under various frequencies, as shown in Figure 1e, assuming that the acoustic pressure difference

of 20 Pa is uniformly distributed over the 0.025 mm thick PTFE membrane with a Young's modulus of 440 MPa. As it can be observed from the simulation results, the deformation regions and magnitudes of the PTFE membrane are highly related to the external sound excitation frequencies, which can be attributed to different resonance frequencies under different vibration modes.

On the other hand, the vibration induced electricity generation is attributed to a coupling effect between contact electrification and electrostatic induction. A cycle of electricity generation process under external pressure is schematically depicted in Figure 1f (see Supporting Information Figure S1 for more details). At its maximum contact state, sound wave induced contact between PTFE and copper will generate electrical charges. The two materials have a different affinity for electrons, with the PTFE attracting electrons from copper, resulting in positive triboelectric charges on the copper side and negative ones on the PTFE side.<sup>30–33</sup> Subsequently, the acoustic pressure will separate the PTFE from copper. As a result, an inner dipole moment between the two contact surfaces is consequently altered, which drives free electrons to flow from the copper electrode on the PTFE membrane to the multihole paper electrode until the maximum separation state is reached. And the free electrons will flow in a reverse direction in the process from maximum separation state toward maximum contact state, which completes a full cycle of electricity generation process.

The electric output of the as-fabricated paper-thin TENG is highly related to the sound wave induced PTFE membrane vibration, while the air damping is acting as a negative impact, of which the influence on acoustic energy harvesting is still underestimated.<sup>34,35</sup> Introducing holes is a rational solution to minimizing the damping but it also reduces the effective contact area as a trade-off. Thus, in order to obtain an optimized output for the paper-thin TENG, arrays of micro holes are added, and the structural parameters of the holes, including shape, dimensions, and distributions, needs also to be systematically optimized.

First, the influence of the hole shape on the output performance is studied at a constant void-to-surface ratio. The transmitting ability of air flow through the holes, namely, the acoustic pressure difference is highly dependent on the hole shapes. As demonstrated in Figure 2a, both the peak distribution and peak values are various with hole shapes. And a best output performance is obtained from the evenly distributed microholes in a circle shape. It is worth noting that, for all the three hole shapes, the frequency-response curves hold a multipack characteristic with all the maximum peak output occurring at ~320 Hz, while the other peaks emerge at the frequencies around the integral multiples of ~80 Hz. This observation is mainly

attributed to that the thin membrane vibrates in a multimodal manner under external acoustic pressure. And each vibration mode holds a natural frequency (see Supporting Information Figure S6 for detailed explanation). At those resonance frequencies, a stable planar standing wave will form over the membrane to cause large deformations, corresponding to the peaks in the frequency-response curves.<sup>36,37</sup>

Second, the center structure is another critical parameter that determines the output performance. Since the added holes on the electrode will reduce the effective contact area, a circular area without holes is purposely reserved in the center of the multihole electrode. As shown in Figure 2b, at a fixed excitation frequency of 320 Hz, the maximum peak output decreases as the hole-free area increases, which is mainly attributed to the weakened membrane vibration due to the air dumping effect in the hole-free part. This also further validates that the air damping is a determining factor for the paper-thin TENG without a resonator.

Third, the influence of the hole diameter on the output performance is also systematically investigated at a constant void-to-surface ratio. As indicated in Figure 2c, experimentally, the peak output is an increasing function of the hole diameter in small hole range until an optimal hole diameter emerges (0.2 mm). And then, the output decreases as the hole diameter increases. Theoretically, the membrane vibration is an increasing function of the air-pressure difference across the PTFE membrane ( $\Delta P_{\text{membrane}}$ ). At a certain sound pressure ( $P_{\text{sound}}$ ),  $\Delta P_{\text{membrane}}$  can be calculated as

$$\Delta P_{\text{membrane}} = P_{\text{sound}} - \Delta P_{\text{hole}} - P_{\text{damping}} \quad (1)$$

where  $P_{\text{damping}}$  is the reduced pressure around PTFE due to air damping. Meanwhile, according to the Hagen–Poiseuille equation,<sup>38</sup> the average air-pressure difference across the multihole electrode ( $\Delta P_{\text{hole}}$ ) can be expressed as

$$\Delta P_{\text{hole}} = 8\mu LQ/(\pi r^4) \quad (2)$$

where  $L$  is the thickness of the multihole electrode,  $\mu$  and  $Q$  are the dynamic viscosity and volumetric flow rate of the air flow, respectively.  $r$  is the average radius of the hole.  $\pi$  is a mathematical constant. According to eqs 1 and 2,  $\Delta P_{\text{hole}}$  increased with the decreasing of the hole diameters, while  $P_{\text{damping}}$  follows a reverse trend. Consequently, an optimal hole diameter will lead to a maximum  $\Delta P_{\text{membrane}}$  thus an optimized output performance.

Fourthly, a further step was taken to study the influence of the void-to-surface ratio of multihole paper electrode on its output performance. As demonstrated in Figure 2d, the electric output is first-increasing and then decreasing function of the void-to-surface ratio and it is maximized at a value of ~20%. A larger void-to-surface ratio will lead to a smaller damping effect of the air, thus, a larger vibration of the PTFE

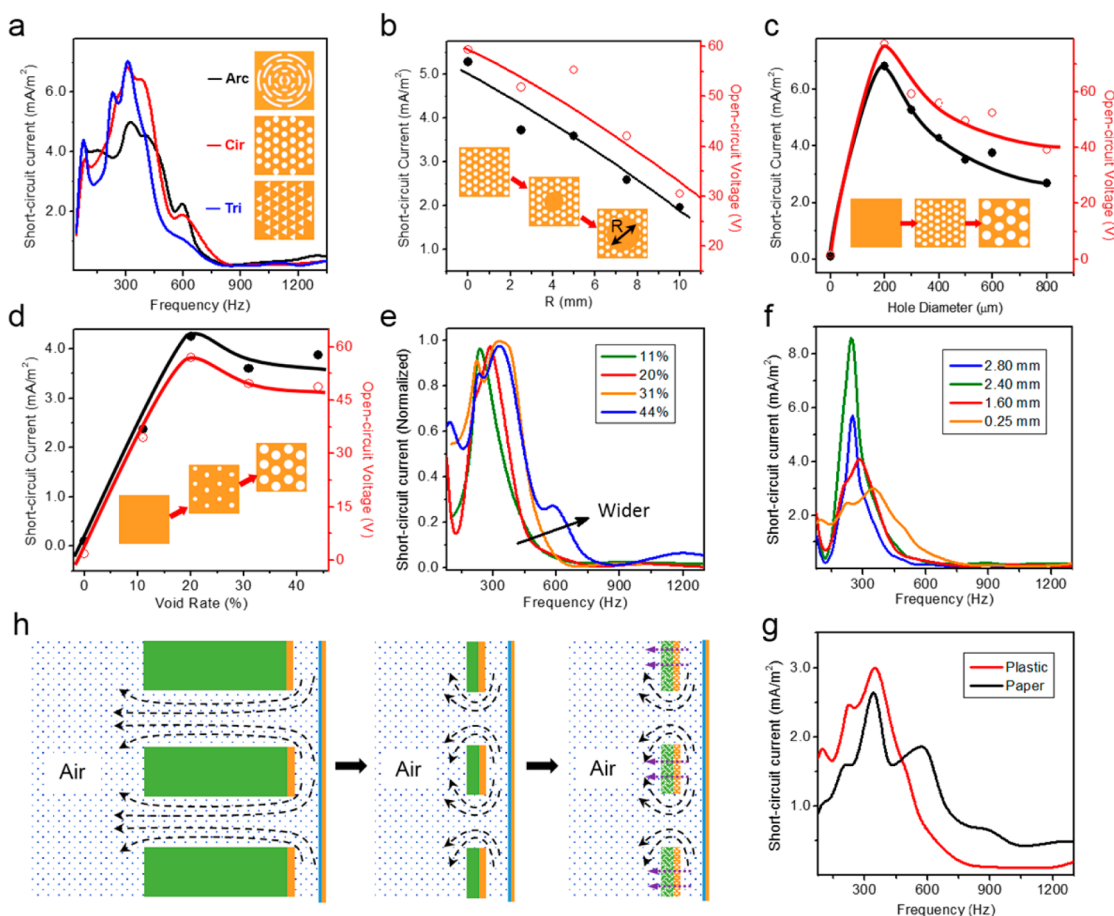


**Figure 2.** Factors that influence the electric output of the triboelectric nanogenerator without Helmholtz resonator. (a) Influence of the hole shapes on the multihole electrode with constant void-to-surface ratio. (b) Influence of the central holes distribution on the electrical output. (c) Influence of hole diameters with constant void-to-surface ratio of 20%. (d) Influence of void-to-surface ratio on the device electrical output. (e) Influence of void-to-surface ratio on the device frequency response. (f) Influence of the electrode thicknesses on the electrical output. (g) Illustration to interpret the influence of the electrode thickness. (h) Influence of electrode substrate materials on the electrical output. All of the measurements were under a constant sound pressure of 120 dB<sub>SPL</sub>.

membrane, however, a smaller effective contact area. The trade-off of larger membrane vibration and smaller effective contact area requires an optimal void-to-surface ratio, as experimentally observed. It is worth noting that the void-to-surface ratio also shows an evident impact on the device working bandwidth, as demonstrated in Figure 2e. As the void-to-surface ratio increases, the frequency response is widened and expanded to a higher frequency range, which is essential to the paper-thin TENG for self-powered active sensing.

Fifthly, the thickness of the multihole electrode is also another important design parameter that needs to be investigated. As shown in Figure 2f, a sharp and narrow output peak was observed for the device with thicker electrode, which is a typical character of a sound-response device based on Helmholtz resonator (see Supporting Information Figure S7 for detailed descriptions). However, the frequency-response curve turns into a broad multipack waveform when the electrode thickness becomes thinner. Especially, the output at a higher frequency ranging up to 700 Hz is obviously

increased with thinner electrode. Theoretically, when the electrode thickness is relatively large, a Helmholtz resonator is formed, which can improve the output at the resonance frequency while narrowing the frequency response range as the trade-off,<sup>39,40</sup> as schematically shown in Figure 2g. Besides, according to eqs 1 and 2,  $\Delta P_{\text{hole}}$  increased with the increasing of the electrode thickness, while  $P_{\text{damping}}$  follows a reverse trend. Thus, there should be an optimized electrode thickness. And a thickness of 2.4 mm is observed experimentally.

Additionally, the paper based multihole electrode is capable of expanding the frequency response, comparing with the plastic sheet based multihole electrode with identical thickness, as indicated in Figure 2h. A possible reason is that the paper holds a micro textile structure with tiny communicating vessels, which would further weaken the air damping effect. In a word, in order to obtain a decent output for the acoustic energy harvester without a resonator, a paper-thin electrode with evenly distributed circular holes is highly desired.

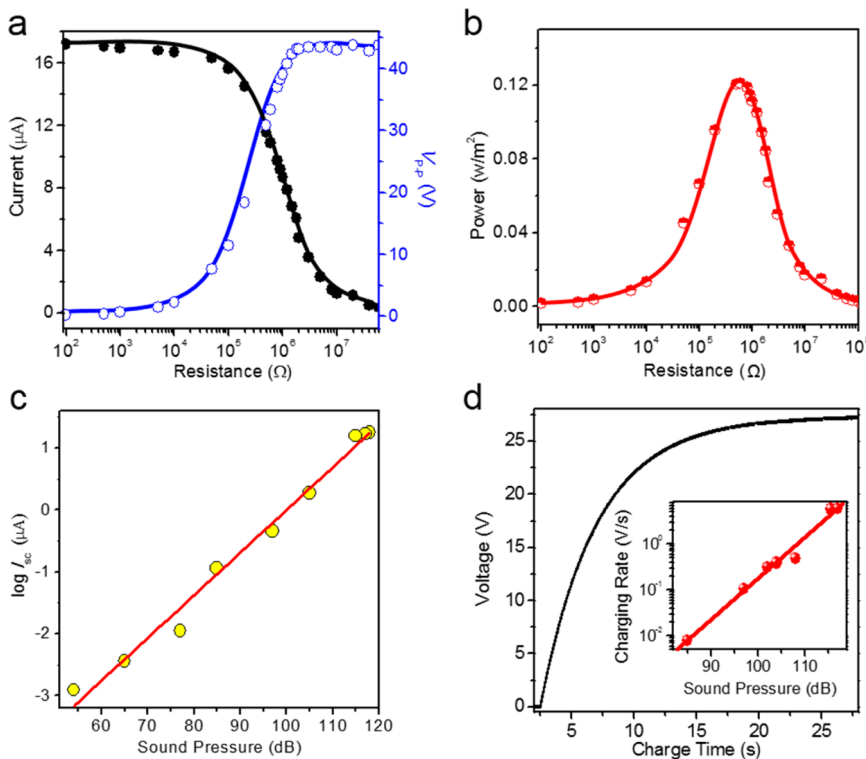


**Figure 3. Electrical output characterization of the paper-based triboelectric nanogenerator. (a)** Dependence of the peak-to-peak voltage ( $V_{p-p}$ ) and current output on the external load resistance. **(b)** Dependence of the peak power output on the resistance of the external load, indicating the maximum power output at  $R = 800 \text{ k}\Omega$ . **(c)** Dependence of the electrical output on the incident sound pressures. **(d)** Charging a  $2 \mu\text{F}$  capacitor under a sound pressure of  $117 \text{ dB}_{\text{SPL}}$  with the sound frequency of  $250 \text{ Hz}$ . Inset is the dependence of charging rate on the incident sound pressure.

Furthermore, resistors were utilized as external loads to further investigate the output power of the structurally optimized paper-thin TENG at the same acoustic condition. Its electric output, including open-circuit voltage and short-circuit current at acoustic frequency of  $250 \text{ Hz}$  with an acoustic pressure of  $114 \text{ dB}_{\text{SPL}}$  was also demonstrated in Supporting Information Figure S2. As displayed in Figure 3a, the voltage amplitudes increase with increasing load resistance, while the current follows a reverse trend owing to the Ohmic loss. As a result, the instantaneous peak power is maximized at a load resistance of  $800 \text{ k}\Omega$ , corresponding to a peak power density of  $121 \text{ mW/m}^2$  (volume power density of  $968 \text{ W/m}^3$ ), as shown in Figure 3b. Furthermore, the dependence of the electrical output on the incident sound pressures was also investigated and a direct proportional function was experimentally observed, as indicated in Figure 3c. Additionally, to quantify the capability of the paper-thin TENG for acoustic energy harvesting, a  $2 \mu\text{F}$  capacitor was charged to  $27 \text{ V}$  in  $15 \text{ s}$  under an acoustic pressure of  $117 \text{ dB}_{\text{SPL}}$  at a frequency of  $250 \text{ Hz}$  (Figure 3d). As the inset indicated, the charging rate is also increasing with the applied sound pressure.

Holding a collection of compelling features, including paper-thin, rollable, broad working bandwidth, and independent of resonator, the proposed nanogenerator demonstrated its unique power in the field of

acoustic energy harvesting. First, it was demonstrated to recycle acoustic energy from a commercial cell phone when playing music (Supporting Information Movie 1) or when a human is talking on the phone (Supporting Information Movie 2). As shown in Figure 4a, the recycled acoustic energy from a cell phone is capable of charging a commercial capacitor up to  $1.8 \text{ V}$  in about  $12 \text{ s}$ . Especially, when the paper-thin triboelectric nanogenerator was installed on a wall or glass window, it can still recycle the environmental noise for electricity generation (Supporting Information Figure S3 and Movie 3). Second, with a broad working bandwidth, the as-fabricated paper-thin TENG is also capable of acting as an active self-powered microphone for sound recording. As demonstrated in Figure 4b and Supporting Information Movie 4, a low-cost ultrathin self-powered microphone was developed, which can efficiently convert the human voice into electrical signals for the recording purpose.

Compared to other existing technologies for acoustic energy harvesting, the paper based TENG distinguishes itself in many aspects and brings about a number of advantages, such as being ultrathin, rollable, low-cost, and environmentally friendly and having extremely high volume power density.

From a structure point of view, the traditional acoustic energy harvester has a bulky structure due to the

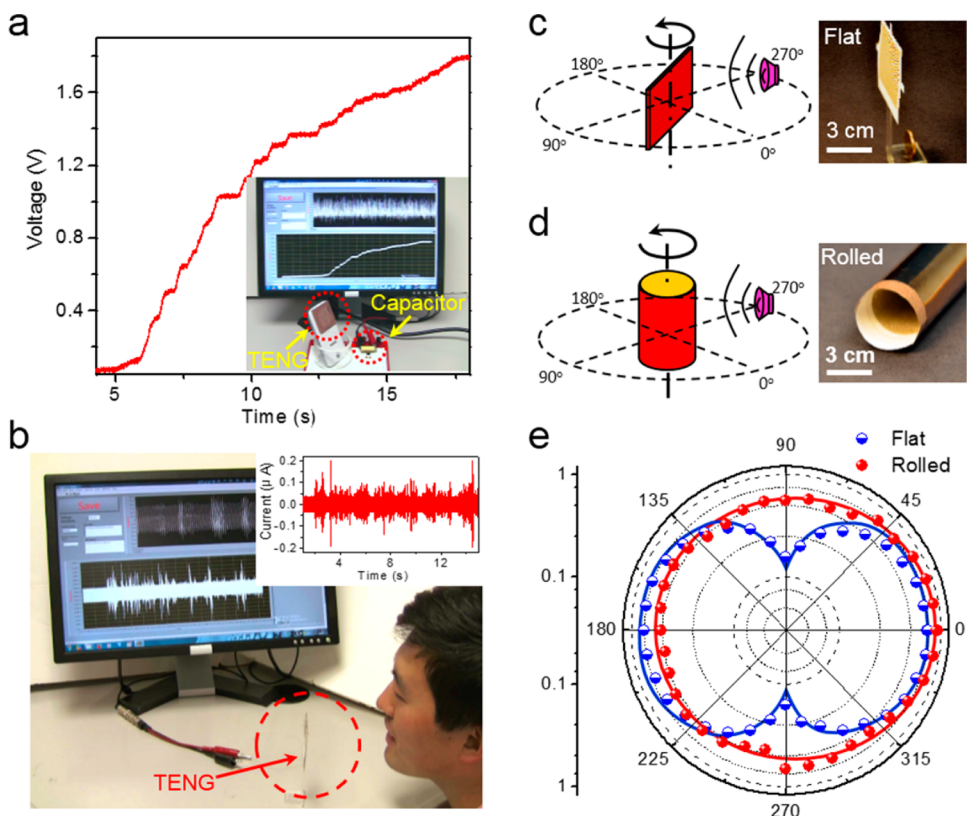


**Figure 4.** Demonstration of the paper-based triboelectric nanogenerator for cell phone sound wave energy harvesting and self-powered sound recording. (a) Recycling the acoustic energy from the cell phone via charging a  $2\ \mu\text{F}$  capacitor. Inset is a photograph that shows a commercial cell phone equipped with a paper-thin triboelectric nanogenerator for capacitor charging. (b) Photograph that shows a paper-thin triboelectric nanogenerator as a self-powered microphone for sound recording. Inset is the acquired electrical signals. Schematic illustrations to show the measurement of the directional patterns of the (c) flat and (d) rolled paper-thin triboelectric nanogenerator. Right sides are the photographs of the as-fabricated device. (e) Shape dependent directional patterns of the paper-based TENG with flat and rolled structure, respectively. (Thanks for Jun Chen's acting as a model for the demonstration.)

requirement of a resonance cavity. Superiorly, the presented ultrathin triboelectric nanogenerator innovatively employs a multi-hole structure on the paper electrode, which effectively eliminates the traditional resonator for acoustic energy harvesting. The paper-thin TENG achieves a volume power density of  $\sim 1\ \text{kW/m}^3$  at a sound pressure of  $117\ \text{dB}_{\text{SPL}}$ .

From the performance point of view, owing to the superior advantages of being structurally ultrathin and flexible, the paper based TENG is rollable. And, for the first time, a novel rolled type device is demonstrated (see Supporting Information Figure S4 for detailed fabrication process). Figure 4c and d displays schematic illustrations to show the measurement of the directional patterns of the flat and rolled paper-thin triboelectric nanogenerator with insets being the photographs of the as-fabricated devices. Figure 4e shows the corresponding shape dependent directional patterns of the TENG with flat and rolled structure, respectively. And a butterfly shaped directional pattern with mirror symmetry was observed for the flat type paper-thin TENG. While the directional pattern of the rolled type is a highly symmetric circle, which indicates the output is independent of the sound wave incident

direction. This is mainly attributed to the rigorous structural symmetry. Holding the advantage of directional independence, the rolled type TENG is suitable to a wide range of circumstances for either energy-harvesting or sensing purposes, such as theatric stage live recording, military surveillance, and omnibearing acoustic energy harvesting.

From a cost point of view, the ultrathin TENG is fabricated mainly based on low-cost, lightweight, and biodegradable paper materials with a simple structure. Besides, based on the surface charging effect, the fabrication requires only very small amount of materials, which are conventional polymers or a thin layer of metal as electrodes. Furthermore, the fabrication process of the paper-thin TENG is straightforward and compatible with possible large-scale manufacturing. Additionally, the backbone of paper-thin TENG is made of commonly used paper materials, which is biodegradable and greatly reduces the possible environmental costs. As a consequence, the paper-based TENG is extremely cost-effective, which is an unparalleled advantage compared to any other acoustic energy harvesting techniques. Importantly, as demonstrated in Supporting Information Figure S5, the paper can be

replaced by transparent organic thin films, and the Cu thin film can be replaced by transparent conductor thin films such as ITO. Therefore, it is entirely feasible to fabricate totally transparent, paper-thin TENGs for harvesting acoustic energy or sound recording, which can be placed at display surface of a cell phone, for example.

## CONCLUSIONS

In summary, we developed the first ultrathin, rollable, paper-based acoustic energy harvester, which innovatively employed the arrays of microholes for acoustic response enhancement. With a thickness of 125  $\mu\text{m}$ , the reported nanogenerator is capable of delivering a maximum power density of 121  $\text{mW/m}^2$  (volume power density of 968  $\text{W/m}^3$ ) under a sound pressure of 117  $\text{dB}_{\text{SPL}}$ . Due to the structural novelty

without a resonator, the device can be implemented onto a commercial cell phone for acoustic energy recycling from human talking, and the electricity generated can charge a capacitor at a rate of 0.144 V/s. An as-prepared paper-based nanogenerator is capable of serving as a self-powered microphone for sound recording. Additionally, owing to the superior advantages of structurally ultrathin and flexible of the paper based TENG, a novel rolled type device is developed. The rigorously structural symmetry enables highly symmetric sound wave response. The concept and design presented in this work can be extensively applied in a variety of other circumstances for either energy-harvesting or sensing purposes, for example, wearable and flexible electronics, military surveillance, jet engine noise reduction, low-cost implantable human ear, and wireless technology applications.

## METHODS

**Fabrication of the Multihole Electrode.** Arrays of small holes with various shapes and distributions were drilled *via* laser-cutting technology (Universal Laser Systems Inc.). The diameter of the smallest hole is 200  $\mu\text{m}$ , which is close to the line-width limitation of the laser cutting on a plate surface. After being polished and cleaned by air blowing, a layer of copper with thickness of 100 nm was deposited onto the multihole electrode *via* physical vapor deposition.

**Nanowire-Based PTFE Surface Modification.** A polytetrafluoroethylene film (25  $\mu\text{m}$  thick) was first washed in series using menthol, isopropyl alcohol, and deionized water. Then, a layer of 100 nm copper was deposited using DC sputter. Subsequently, the aligned nanowires on the PTFE surface were obtained *via* an inductively coupled plasma (ICP) reactive ion etching process. And O<sub>2</sub>, Ar, and CF<sub>4</sub> gases were injected into the ICP chamber with a flow ratio of 10.0, 15.0, and 30.0 sccm, respectively. A large density of plasma was produced by a power source of 400 W, and another power source of 100 W was used to accelerate the plasma ions.

**Experimental Setup for Electric Measurement.** A loudspeaker (Fostex Inc.) that provides sinusoidal sound waves was used as an acoustic source with tunable frequency and amplitude. A sound level meter (Extech Inc.) with 2 dB accuracy and 0.1 dB resolution was used to measure the incident acoustic pressure. The meter was located near the harvester at a distance far less than the acoustic wavelength.

**Conflict of Interest:** The authors declare no competing financial interest.

**Supporting Information Available:** Demonstration of the electricity generation process; electrical measurement results of a paper-based TENG; recycling the environmental noise to generate power; fabrication process of a rolled-type paper-thin TENG; a transparent, paper-thin TENG; the paper-based TENG acting as a portable acoustic energy harvester and a self-powered acoustic sensor, as Movies S1–S4. This material is available free of charge *via* the Internet at <http://pubs.acs.org>.

**Acknowledgment.** This work was supported by the High-tower Foundation, the “Thousands Talents” program for pioneering researchers and their innovation team, China.

## REFERENCES AND NOTES

- Li, C. W.; Ciston, J.; Kanan, M. W. Electroreduction of Carbon Monoxide to Liquid Fuel on Oxide-Derived Nanocrystalline Copper. *Nature* **2014**, *508*, 504–507.
- Peng, Q.; Tanaka, S.; Ito, S.; Tetreault, N.; Manabe, K.; Nishino, H.; Nazeeruddin, M. K.; Grätzel, M. Inorganic Hole Conductor-Based Lead Halide Perovskite Solar Cells with 12.4% Conversion Efficiency. *Nat. Commun.* **2014**, *5*, 3834.
- Wang, Z. L.; Song, J. Piezoelectric Nanogenerators Based on Zinc Oxide Nanowire Arrays. *Science* **2006**, *312*, 242–246.
- Pasta, M.; Wessells, C. D.; Liu, N.; Nelson, J.; McDowell, M. T.; Huggins, R. A.; Toney, M. F.; Cui, Y. Full Open-Framework Batteries for Stationary Energy Storage. *Nat. Commun.* **2014**, *5*, 3007.
- Qin, Y.; Wang, X. D.; Wang, Z. L. Microfibre–Nanowire Hybrid Structure for Energy Scavenging. *Nature* **2008**, *451*, 809–813.
- Zhu, G.; Su, Y.; Bai, P.; Chen, J.; Jing, Q.; Yang, W.; Wang, Z. L. Harvesting Water Wave Energy by Asymmetric Screening of Electrostatic Charges on a Nanostructured Hydrophobic Thin-Film Surface. *ACS Nano* **2014**, *8*, 6031–6037.
- Cha, S. N.; Seo, J. S.; Kim, S. M.; Kim, H.; Park, Y. J.; Kim, S.; Kim, J. M. Sound-Driven Piezoelectric Nanowire-Based Nanogenerators. *Adv. Mater.* **2010**, *22*, 4726–4730.
- Que, R. H.; Shao, Q.; Li, Q. L.; Shao, M. W.; Cai, S.; Wang, S. D.; Lee, S. T. Flexible Nanogenerators Based on Graphene Oxide Films for Acoustic Energy Harvesting. *Angew. Chem., Int. Ed.* **2012**, *124*, 5514–5518.
- Yang, J.; Chen, J.; Liu, Y.; Yang, W.; Su, Y.; Wang, Z. L. Triboelectrification-Based Organic Film Nanogenerator for Acoustic Energy Harvesting and Self-Powered Active Acoustic Sensing. *ACS Nano* **2014**, *8*, 2649–2657.
- Yang, J.; Chen, J.; Su, Y.; Jing, Q.; Li, Z.; Yi, F.; Wen, X.; Wang, Z.; Wang, Z. L. Eardrum-Inspired Active Sensors for Self-Powered Cardiovascular System Characterization and Throat-Attached Anti-interference Voice Recognition. *Adv. Mater.* **2015**, *27*, 1316–1326.
- Smoker, J.; Nouh, M.; Aldraihem, O.; Baz, A. Energy Harvesting from a Standing Wave Thermoacoustic-Piezoelectric Resonator. *J. Appl. Phys.* **2012**, *111*, 104901.
- Wu, L. Y.; Chen, L. W.; Liu, C. M. Acoustic Energy Harvesting Using Resonant Cavity of a Sonic Crystal. *Appl. Phys. Lett.* **2009**, *95*, 013506.
- Hu, X. H.; Ho, K. M. Homogenization of Acoustic Metamaterials of Helmholtz Resonators in Fluid. *Phys. Rev. B* **2008**, *77*, 172301.
- Cervenka, M.; Soltes, M.; Bednark, M. Optimal Shaping of Acoustic Resonators for the Generation of High-Amplitude Standing Waves. *J. Acoust. Soc. Am.* **2014**, *136*, 1003–1012.
- Chen, J.; Zhu, G.; Yang, J.; Jing, Q.; Bai, P.; Yang, W.; Qi, X.; Su, Y.; Wang, Z. L. Personalized Keystroke Dynamics for

- Self-Powered Human-Machine Interfacing. *ACS Nano* **2015**, *9*, 105–116.
16. Yang, W.; Chen, J.; Wen, X.; Jing, Q.; Yang, J.; Su, Y.; Zhu, G.; Wu, W.; Wang, Z. L. Triboelectrification Based Motion Sensor for Human-Machine Interfacing. *ACS Appl. Mater. Interfaces* **2014**, *6*, 7479–7484.
  17. Zhang, H.; Yang, Y.; Su, Y.; Chen, J.; Adams, K.; Lee, S.; Hu, C.; Wang, Z. L. Triboelectric Nanogenerator for Harvesting Vibration Energy in Full Space and as Self-Powered Acceleration Sensor. *Adv. Funct. Mater.* **2014**, *24*, 1401–1407.
  18. Li, Z.; Chen, J.; Yang, J.; Su, Y. J.; Fan, X.; Wu, Y.; Yu, C.; Wang, Z. L.  $\beta$ -Cyclodextrin Enhanced Triboelectrification for Self-Powered Phenol Detection and Electrochemical Degradation. *Energy Environ. Sci.* **2015**, *8*, 887–896.
  19. Su, Y.; Zhu, G.; Yang, W.; Yang, J.; Chen, J.; Jing, Q.; Wu, Z.; Jiang, Y.; Wang, Z. L. Triboelectric Sensor for Self-Powered Tracking of Object Motion Inside Tubing. *ACS Nano* **2014**, *8*, 3843–3850.
  20. Chen, J.; Yang, J.; Li, Z.; Fan, X.; Zi, Y.; Jing, Q.; Guo, H.; Wen, Z.; Pradel, K. C.; Niu, S.; Wang, Z. L. Networks of Triboelectric Nanogenerators for Harvesting Water Wave Energy—A Potential Approach Toward Blue Energy. *ACS Nano* **2015**, *9*, 3324–3331.
  21. Zhu, G.; Chen, J.; Zhang, T.; Jing, Q.; Wang, Z. L. Radial-Arrayed Rotary Electrification for High Performance Triboelectric Generator. *Nat. Commun.* **2014**, *5*, 3426.
  22. Yang, J.; Chen, J.; Yang, Y.; Zhang, H.; Yang, W.; Bai, P.; Su, Y.; Wang, Z. L. Broadband Vibrational Energy Harvesting Based on a Triboelectric Nanogenerator. *Adv. Energy Mater.* **2014**, *4*, 1301322.
  23. Chen, J.; Zhu, G.; Yang, W.; Jing, Q.; Bai, P.; Yang, Y.; Hou, T. C.; Wang, Z. L. Harmonic-Resonator-Based Triboelectric Nanogenerator as a Sustainable Power Source and a Self-Powered Active Vibration Sensor. *Adv. Mater.* **2013**, *25*, 6094–6099.
  24. Bai, P.; Zhu, G.; Jing, Q.; Yang, J.; Chen, J.; Su, Y.; Ma, J.; Zhang, G.; Wang, Z. L. Membrane-Based Self-Powered Triboelectric Sensors for Pressure Change Detection and Its Uses in Security Surveillance and Healthcare Monitoring. *Adv. Funct. Mater.* **2014**, *24*, 5807–5813.
  25. Yang, W.; Chen, J.; Jing, Q.; Yang, J.; Wen, X.; Su, Y.; Zhu, G.; Bai, P.; Wang, Z. L. 3D Stack Integrated Triboelectric Nanogenerator for Harvesting Vibration Energy. *Adv. Funct. Mater.* **2014**, *24*, 4090–4096.
  26. Zhu, G.; Bai, P.; Chen, J.; Wang, Z. L. Power-Generating Shoe Insole Based on Triboelectric Nanogenerators for Self-Powered Consumer Electronics. *Nano Energy* **2013**, *2*, 688–692.
  27. Yang, W.; Chen, J.; Zhu, G.; Wen, X.; Bai, P.; Su, Y.; Lin, Y.; Wang, Z. L. Harvesting Vibration Energy by a Triple-Cantilever Based Triboelectric Nanogenerator. *Nano Res.* **2013**, *6*, 880–886.
  28. Zhu, G.; Chen, J.; Liu, Y.; Bai, P.; Zhou, Y. S.; Jing, Q.; Pan, C.; Wang, Z. L. Linear-Grating Triboelectric Generator based on Sliding Electrification. *Nano Lett.* **2013**, *13*, 2282–2289.
  29. Yang, W.; Chen, J.; Zhu, G.; Yang, J.; Bai, P.; Su, Y. J.; Jing, Q.; Cao, X.; Wang, Z. L. Harvesting Energy from the Natural Vibration of Human Walking. *ACS Nano* **2013**, *7*, 11317–11324.
  30. Fan, F. R.; Tian, Z. Q.; Wang, Z. L. Flexible Triboelectric Generator. *Nano Energy* **2012**, *1*, 328–334.
  31. Hou, T. C.; Yang, Y.; Zhang, H.; Chen, J.; Chen, L. J.; Wang, Z. L. Triboelectric Nanogenerator Built inside Shoe Insole for Harvesting Walking Energy. *Nano Energy* **2013**, *2*, 856–862.
  32. Zhu, G.; Zhou, Y. S.; Bai, P.; Meng, X. S.; Jing, Q.; Chen, J.; Wang, Z. L. A Shape-Adaptive Thin-Film-Based Approach for 50% High-Efficiency Energy Generation through Micro-Grating Sliding Electrification. *Adv. Mater.* **2014**, *26*, 3788–3796.
  33. Zhang, H.; Yang, Y.; Su, Y.; Chen, J.; Hu, C.; Wu, Z.; Liu, Y.; Wong, C. P.; Bando, Y.; Wang, Z. L. Triboelectric Nanogenerator as Self-powered Active Sensors for Detecting Liquid/Gaseous Water/Ethanol. *Nano Energy* **2013**, *2*, 693–701.
  34. Yu, K.; Zijlstra, P.; Sader, J. E.; Xu, Q. H.; Orrit, M. Damping of Acoustic Vibrations of Immobilized Single Gold Nanorods in Different Environments. *Nano Lett.* **2013**, *13*, 2710–2716.
  35. Zhou, J.; Bhaskar, A.; Zhang, X. The Effect of External Mean Flow on Sound Transmission through Double-Walled Cylindrical Shells Lined with Poroelastic Material. *J. Sound Vibr.* **2014**, *333*, 1972–1990.
  36. Goll, E.; Dalhoff, E. Modeling the Eardrum as a String with Distributed Force. *J. Acoust. Soc. Am.* **2011**, *130*, 1452–1462.
  37. Kashy, E.; Johnson, D. A.; McIntyre, J.; Wolfe, S. L. Transverse Standing Waves in a String with Free Ends. *Am. J. Phys.* **1997**, *65*, 310–313.
  38. Holt, J. K.; Park, H. G.; Wang, Y.; Stadermann, M.; Artyukhin, A. B.; Grigopoulos, C. P.; Noy, A.; Bakajin, O. Fast Mass Transport through Sub-2-nanometer Carbon Nanotubes. *Science* **2006**, *312*, 1034–1037.
  39. Han, F. S.; Seiffert, G.; Zhao, Y. Y.; Gibbs, B. Acoustic Absorption Behaviour of an Open-Celled Aluminium Foam. *J. Phys. D: Appl. Phys.* **2003**, *36*, 294–302.
  40. Murray, A. R. J.; Summers, I. R.; Sambles, J. R.; Hibbins, A. P. An Acoustic Double Fishnet Using Helmholtz Resonators. *J. Acoust. Soc. Am.* **2014**, *136*, 980–984.